Heliyon 9 (2023) e17412

Contents lists available at ScienceDirect

Heliyon

journal homepage: www.cell.com/heliyon

Monitoring of drainage system and waterlogging area in the human-induced Ganges-Brahmaputra tidal delta plain of Bangladesh using MNDWI index

Md. Bazlar Rashid

Geological Survey of Bangladesh, 153- Pioneer Road, Segunbagicha, Dhaka, 1000, Bangladesh

ARTICLE INFO

Keywords:
Bengal delta coast
River morphology
MNDWI

ABSTRACT

Waterlogging is one of the major global problems which affects agro-economic activities around the world. In the coastal areas of Bangladesh, especially the southwestern coast, drainage congestion and waterlogging are very common which makes the area uninhabitable. Therefore, timely checking of drainage systems and surface water, and conveying data on the dynamics of drainages and surface water are important for plan and supervisory processes. The present study took an effort to illustrate the waterlogging and morphological change of the rivers in the southwestern coast of Bangladesh through the Modification Normalized Difference Water Index (MNDWI) values which are valuable indicators for monitoring the water area and land use pattern change. Landsat images (Landsat L8 Oli TIRS, Landsat ETM+, Landsat TM) were used in the research. The study reveals that from 1989 to 2020, the shallow water area (mostly covered with rivers) decreased by ~14.30 km^2 yr^{-1}, whereas the wet-land area (mostly covered with *beels* and water logging areas) increased by ~ 67.12 km^2 yr^{-1}. The bare land area also increased at a rate of ~ 36.90 km^2 yr^{-1}. On the other hand, the green vegetation decreased at a rate of ~166.1 km^2 yr^{-1}, whereas the moderate green vegetation area increased by ~ 69.77 km^2 yr^{-1} for the same period. In the coastal zones of Bangladesh, the polders, embankments, upstream dams, etc., enhance more sedimentation within the channels rather than in the nearby tidal plains. As a result, the shallow water area which is mostly covered by rivers is gradually decreasing. Moreover, due to increase in wet-land areas with salinity intrusions which affect the vegetation. Therefore, the green vegetation area is regularly declining due to demolition or conversion to moderate green vegetation. The findings of the research will be supportive for coastal scientists worldwide, policy makers & planners, and finally supportive for sustainable management of the coastal areas including Bangladesh.

1. Introduction

Waterlogging due to both natural (climate change, sea level rise, etc.) and anthropogenic (polders, embankments, upstream dams, etc.) processes is one of the major global problems which has affected the agro-economic activities around the world [1–3]. The troubles of waterlogging are well recognized and studied, but still it continues in most parts of the world [4–6]. In the coastal zones of Bangladesh (Fig. 1), saline water imposition and tidal flooding hampered agricultural practices [7–9]. Therefore, from 1960s to 1980s ~ 5000 km^2 area was protected from tidal flooding and saline water by the construction of ~ 139 polders of ~ 4000 km lengths [10,11],

E-mail address: bazlarrashid@ymail.com.

https://doi.org/10.1016/j.heliyon.2023.e17412
Received 31 January 2023; Received in revised form 14 June 2023; Accepted 15 June 2023
Available online 21 June 2023

and also constructed embankments on both the banks of the tidal rivers [12]. But after a few years, other problems appeared in the areas i.e. channel sedimentation, drainage congestion, land subsidence, waterlogging, etc. [12–14]; Fig. 2). Due to embankments along both banks of the tidal channels and poldering around the tidal plain areas, the sedimentation is not taking place in the plain lands. It is mainly taking place within the channels (Fig. 2a). Therefore, drainage congestion and drainage abandonment are very common in the areas due to excess sedimentation within the channels (Fig. 2a,d,e). Rivers play a role in carrying water with sediments, and eventually in building landmasses. It also plays the role of fish production, transportation, power generation, irrigation, etc. Therefore, the morphological transforms in any river can influence sediment transport ability and water release, and accordingly affect the morphology of an area [15–19]. On the other hand, due to the lack of sedimentation of the tidal plain areas, the plain lands gradually subsided in respect to the sea level due to deficit of sedimentation and compaction of loose delta sediments [19,20]. Rashid et al. [13] stated that the channels of the area lost about 5–8 m widths yr^{-1}, and consequently ~ 6000 km of waterways were lost in the last few decades [11]. Due to drainage congestion or silting of many rivers, the rivers cannot carry the surplus water during the monsoon, and

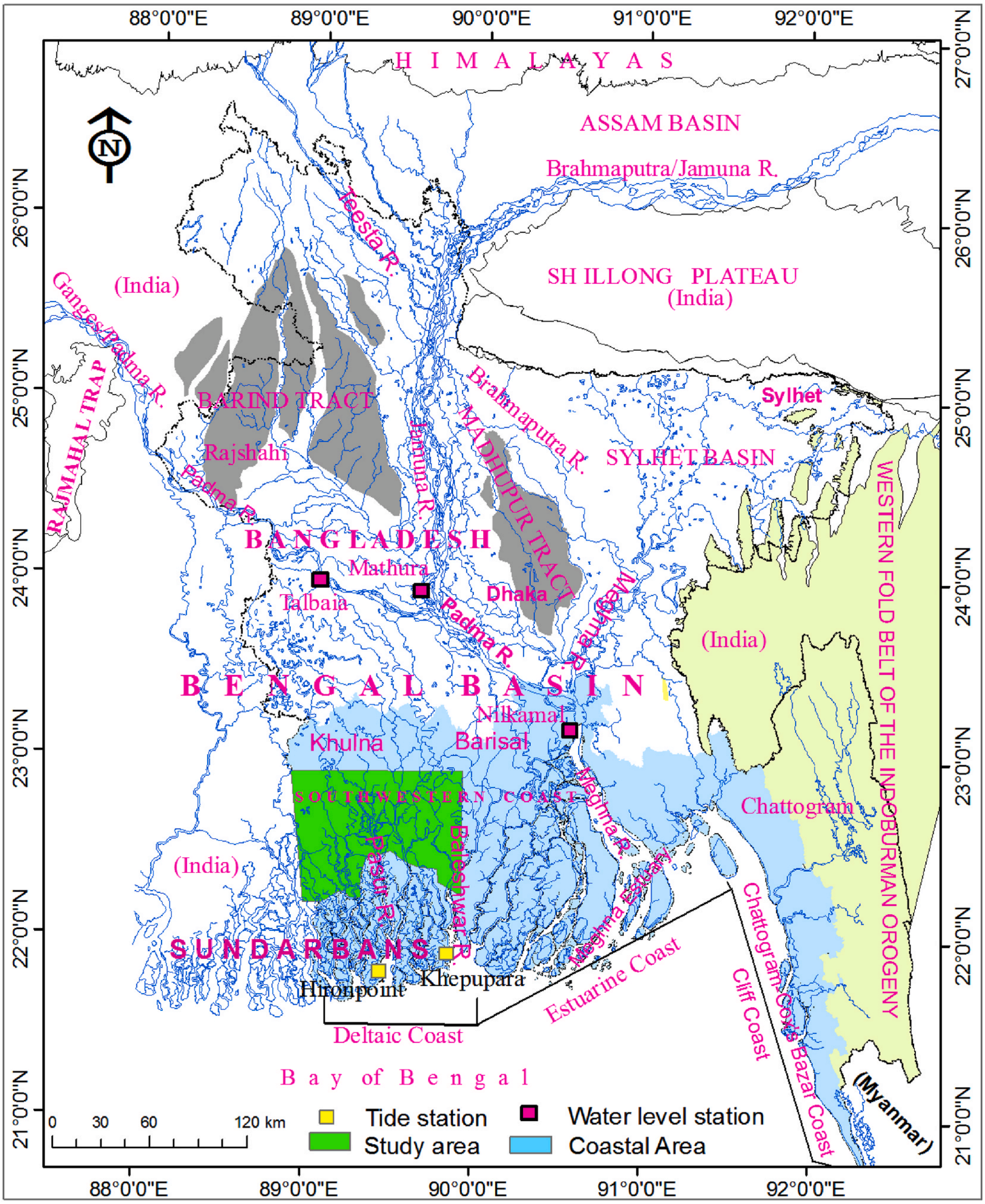

Fig. 1. Major physiographic features of the Bengal Basin, Bangladesh coast and study area.

Fig. 2. A) The silted Kabodak River at Baradal Asasuni, Satkhira District; (b) inundation of Khulna-Satkhira Highway due to flooding at Noapara, Tala, Satkhira District; c) waterlogging at Pratapnagar, Asasuni, Satkhira District due to Cyclone Amphan; d) Google Images 2021 showing silted tributary channel of Rupsha River at Batiaghata, Khulna District; e) silted tributary channel of Atharobaki River, Rupsha, Khulna District; f) water logging at Gopinathpur of Kalaroya Upazilla, Satkhira District.

water overtops the banks. Therefore, waterlogging and drainage congestion in the southwestern (SW) coastal part of Bangladesh have increased rapidly in recent decades (Fig. 2b,c,f). Rashid et al. [12] found that from 1978 to 2011 the waterlogging area was increasing at a rate of ~ 31 km^2 yr^{-1}. Therefore, regular and consistent measurements of the waterlogging area and drainage system change are essential to monitor the dynamic altars of the water area and drainage systems for sustainable management of the area.

Water body delineation is a significant task in various disciplines, such as erosion monitoring, coastline change, coastal zone management, flood forecast, assessment of water resources, etc. [21]. Timely checking of drainage systems and surface water, and conveying data on the dynamics of drainages and surface water are important for plan and supervisory processes [22]. With the beginning of satellite remote sensing technology, it becomes likely to sense, map, and supervise the drainage system and waterlogged areas more competently and reasonably [6,23–28]. Spectral indices derived from multispectral remotely sensed images based on MNDWI (Modification Normalized Difference Water Index) [29–34] are used to illustrate water bodies, landform patterns, and ecological study, respectively, and it is a powerful index [35–40]. Although, different researches conducted about sedimentation, tidal river siltation, drainage congestion, waterlogging, tidal river supervision, etc., in the Ganges-Brahmaputra-Meghna (GBM) tidal delta plain [19,41–47]. However, till now the morphological changes of the rivers and waterlogging areas in the SW coastal zones of Bangladesh have not been sincerely addressed by using this technique. Earlier studies of the waterlogging area and drainage systems were based on manual digitization and visual interpretation of satellite data [12] interpretation. So, to evaluate the patterns of waterlogging areas and drainage systems that have changed over the last few decades, in addition to the gaps in this research, the author applied MNDWI analysis to identify increasing trends in the waterlogging area in specified time intervals as well as drainage system investigation. The main objectives of the study were: (1) to delineate the changes in tha shallow water area and morphology of rivers, (2) to illustrate the changes in waterlogging areas, and (3) to exemplify the alters in vegetation patterns of the area. The innovation of the study was to illustrate river morphology, water logging areas and vegetation patterns change in the SW coastal zones of Bangladesh in the past few decades through widely accepted Geographic Information System and Remote Sensing (RS) based MNDWI index analysis, and throw the message to the national and international communities to understand the real scenario of SW coastal part of Bangladesh. Definitely, the results of the study will be useful to realize the actual situation of the SW coastal part of the country and ultimately to the policy-makers, planners, and coastal scientists all over the globe to take necessary measures for the sustainable management of the coastal zone. Finally, it will help to protect the coastal areas from such undesirable situations.

2. Data and methodology

2.1. Study area

The GBM delta is one of the biggest deltas in the globe. This delta includes a major part of the Bengal basin. The delta continues to the south and finally falls into the Bay of Bengal (BoB). Before entering the bay, it created a wide coastal area (Fig. 1). The present research area is situated in the SW coastal zone of Bangladesh. The area is covered with fluvio-tidal to tidal deposits [47,48]. In general, the slope of the region is towards SSE, and smoothly slopes to the BoB in the south. The area is generally smooth with an average elevation of ~ 2 m above sea level. The region includes subtropical monsoon climates, with temperatures ranging from 12 to 35 °C and monthly rainfall varying from 7 to 345 mm (Fig. 3a–c).

2.2. Data source

The multi-temporal Landsat images were downloaded from the USGS website (http://glovis.usgs.gov) which represents 2020, 2014, 2000 and 1989 (Table 1). During the monsoon (June to October) the subcontinent experiences heavy rainfall (Fig. 3b and c), which causes flooding in these areas, inundation of low-lying areas and high-water levels in rivers (Fig. 4). Therefore, satellite images obtained during the monsoon season are not suitable for waterlogging analysis. Therefore, the dry period (November to May) (Fig. 3a–c) images were considered for analysis, clear with a cloudless and spatial resolution of 30 m. The images used for water content analysis, it is also necessary to confirm that these are collected with approximately similar tidal water level conditions as practically big tidal arrays are observed along the coast of Bangladesh [11]). Thus, tidal water levels of all used images were confirmed by the tidal records of Khepupara and Hiron Point Tide gauge stations (locations can be seen in Fig. 1) of Bangladesh Inland Water Transport Authority (BIWTA). Approximately similar water stages were considered to choose the images, though have several deviations (Table 1) due to unavailability of clear images at regular gaps and similar tidal conditions. Consequently, the temporary ranges of images were varied in different periods and years.

2.3. Image preprocessing

The images (Table 1) were pre-processed to recover and assess information from remotely sensitive records (Fig. 5). Image mosaics and radiometric corrections were completed through Erdas Imagine 2014 software. ArcMap 10.2 was applied to draw out the desired area through the Spatial Analyst tool (Mask). Landsat TM, Landsat ETM+ and Landsat L8 Oli TIRS multispectral sensors have bands

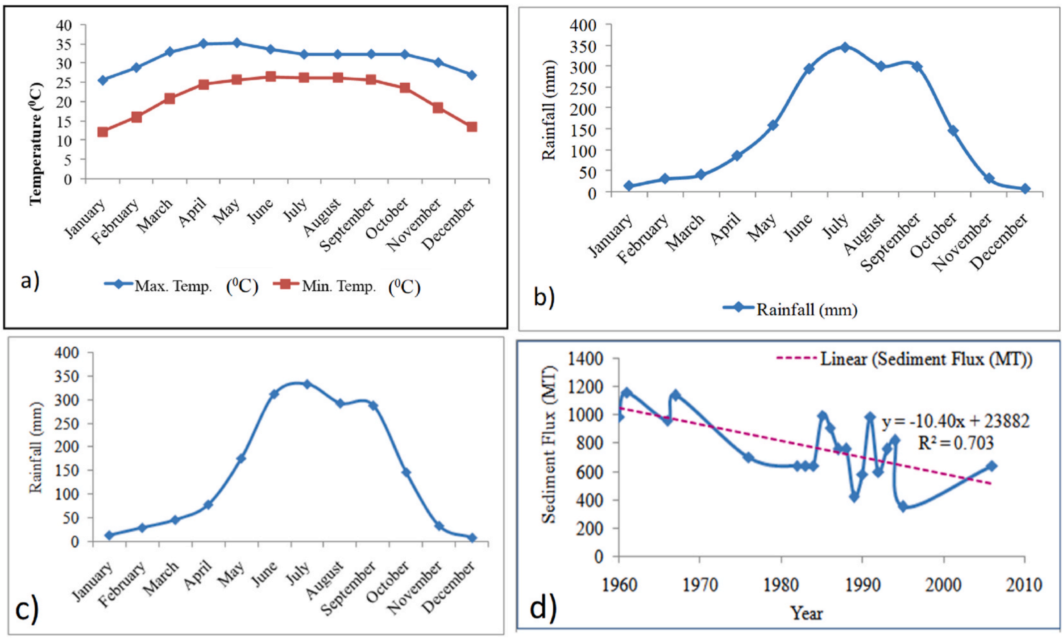

Fig. 3. A) Average monthly maximum and minimum temperature, b) average monthly rainfall, and c) average monthly rainfall from 1981 to 2010 in the study area (Source: Bangladesh Meteorological Department (BMD)); d) sediment flux in million ton (MT) in the GBM system (Source: BWDB).

Table 1
Landsat images used in the study.

Satellite Sensor/ SPACECRAFT_ID	Acquisition Date and time (GMT)	Spatial resolution (m)	Path/ Row	No. Of Band	Data Type	Tide level (m)	Tide station
TM	February 21, 1989 3:54 a.m.	30	137/044	7	Ver 1.0	2.1	Hiron point
	February 28, 1989 4:00 a.m.		138/044			1.6	Hiron point
ETM+	January 19, 2000 3:59 a.m.	30	137/044	7	L1G	2.0	Hiron point
	January 26 2000 4:05 a.m.		138/044			1.6	Hiron point
L8 OLI TIRS	January 25, 2014 4:26 a.m.	30	137/044	11	L1T	1.36	Khepuparat
	March 05 2014 4:31 a.m.		138/044			2.5	Hiron point
L8 OLI TIRS	February 11, 2020 4:24 a.m.	30	137/044	11	L1TP	2.3	Hiron point
	February 02, 2020 4:31 a.m.		138/044			2.2	Hiron point

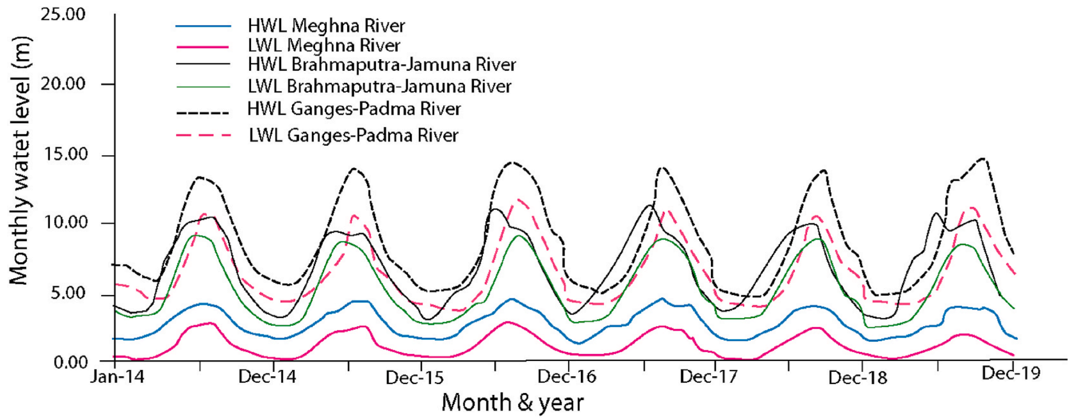

Fig. 4. Monthly highest and lowest water level of Ganges-Padma River (Talbaria, Bangladesh Water Development Board (BWDB), Station ID-SW91), Brahmaputra-Jamuna River (Mathura, BWDB, Station ID- SW50.3) and Meghna River (Nilkamal, BWDB, Station ID- SW277.3) during January- 2014 to December- 2019 (See Fig. 1 for station location).

like short-wave infrared, near infrared, red, and green (bands 5, 4, 3, and 2) applied to draw out various characteristics. The images were projected at UTM with zones 45 N and 46 N, and WGS 84 datum.

2.4. MNDWI analysis

Ideal drainage system with appropriate bathymetry, discharge capacity, interconnectedness with tidal flats, etc., is an important parameter in any coastal process such as sediment transport, estuarine circulation, delta morphology, etc. [12,13,19,20]. Traditionally, bathymetric data were collected from depth soundings made by boats. But, boat-based estimates are restricted to ship paths, and missing distant and shallow waters [49]. Airborne bathymetric LiDAR is promising one of the leading technologies for generating high-resolution digital landscape models for shallow water environments [49]. However, LiDAR is still expensive for large-scale investigations. Similarly, drones with fluid lensing and structure-from-motion (SFM) technologies [50] facilitate centimeter-scale resolution [51] bathymetric mapping. But drone investigations are limited to comparatively small areas due to battery restrictions of quadcopters and fixed-wing remote-controlled aerial vehicles. Recently, many researchers have used physics-based algorithms and spectral analysis to describe water depth, and derive water depth from satellite images [52,53]. However, in all these cases ground truth data are important for describing shallow-water depths [54]. In the present study, spectral based MNDWI is used to obtain an idea of shallow water depth in the SW coastal part of Bangladesh. Moreover, ground truth data/experience is also used to validate the results (Fig. 2).

MNDWI is a distant sensing-based indicator applied to investigate the composition of water [30,53,55,56]. It is an important indicator for supervising drought, water stress, soil erosion, etc. [39,40]. It is limitless, and its values are between - 1 and + 1. High values stand for elevated water content or high-water depth, and low values reflect low water content or low water depth [53,57]. Xu [30] proposed to calculate MNDWI using the following equation;

$$\mathrm{MNDWI} = (\mathrm{GREEN} - \mathrm{SWIR}) \ / \ (\mathrm{GREEN} + \mathrm{SWIR})$$

GREEN is the indication in the green array spectrum and SWIR is the short-wave infrared spectrum. MNDWI was executed by Archmap 10.2's Spatial Analyzer tool through Raster Calculator.

In terms of precision with deliberation of various classification methods, the band ratios supervised classification is better [58]. The whole research area was divided into five categories as shallow water (mostly covered with rivers), wet-land (mostly covered with *beels*

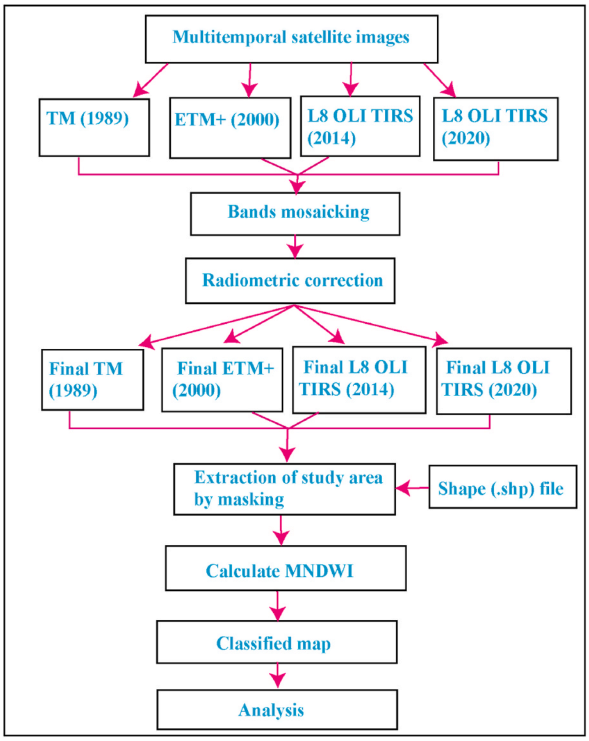

Fig. 5. Methodology for the present study.

and water logging areas), moderate green vegetation, bare land, and green vegetation based on MNDWI index (Table 3). After extracting the different classes, it is reclassified by the Spatial Analyst tool of Archmap 10.2's, and the area of various classes is calculated by the Field Calculator tool of the same software from the Attribute table.

2.5. Validation of MNDWI classification maps

The land exercises of the coastal areas are remarkably multifaceted. Therefore, accuracy estimation is important for individual classification for the assessment of land use alters [59]. In this research classification precision was conducted by evaluation of each classification outcome with suggestion data acquired from Landsat imageries by visual image explanation through different band arrangements [16–18,60,61] and field investigation (Fig. 2). Manual visual image explanation (MVIE) is of utmost significance for almost all quantitative performance evaluations [62], especially to unveil the potency of instrument learning algorithms. It is generally established in the text that MVIE plays an important role in reliable geodata [16–18,60,61]. But it depends on the knowledge of the analyst, the image quality, etc. [60,62]. MVIE is often used as a reference for automatic procedures and rationale since it is still being seen as a methodology, resulting in acceptable accuracies [60,62]. Hence, the classification precision of digital image categorization was assessed by evaluating each classification outcome with reference data gained from visual analysis and field examinations (Fig. 2). Many researchers also extracted data from Google Earth images and utilized them for precision evaluation [59]. The equations of user accuracy, producer accuracy, overall accuracy, and Kappa statistics are some of the finest quantitative evaluations [63] of satellite image classification given below:

$$\text{User Accuracy} = \frac{\text{Number of corrected classified pixels in each category}}{\text{Total number of Reference Pixels in each category (The Row Total)}} \times 100 \tag{1}$$

$$\text{Producer Accuracy} = \frac{\text{Number of corrected classified pixels in each category}}{\text{Total number of Reference Pixels in each category (The Column Total)}} \times 100 \tag{2}$$

$$\text{Overall Accuracy} = \frac{\text{Total number of corrected classified pixels (Diagonal)}}{\text{Total number of reference pixels}} \times 100 \tag{3}$$

$$\text{Kappa Coefficient (T)} = \frac{\text{(Total sample x Total corrected sample)} - \sum\text{(column total x Row total)}}{\text{(Total number of samples)}^2 - \sum\text{(column total x Row total)}} \times 100 \tag{4}$$

3. Results

3.1. MNDWI classification and precision evaluation

The land cover classification map was prepared from Landsat images using the MNDWI index values for the years 1989 (Fig. 6a), 2000 (Figs. 6b), 2014 (Fig. 6c), and 2020 (Fig. 6d), shown in Fig. 6. The classified MNDWI maps precision estimation using Kappa statistics, overall accuracy, user accuracy and producer accuracy are presented in Table 2. The overall classification precision of produced maps was documented as 75.0%, 77.5%, 80.0%, and 82.5% for 1989, 2000, 2014, and 2020, respectively. The overall accuracy results show that confirmation rates for all years were greatly higher than 75%, representing a good precision conformity for classification [64]. Furthermore field visit experience was used to confirm the accuracy assessment (Fig. 2).

3.2. Land use pattern and water content area change over 1989 to 2020

The spatiotemporal changes in waterlogging and drainage systems from 1989 to 2020 are examined based on satellite-derived water body extraction index (MNDWI) using Landsat TM, ETM+, and L8 OLI TIRS data. The accuracy assessment was done through manual visual image explanation (MVIE) and field surveys. The MNDWI index is an excellent indicator to recognize water area alter [30,53]. In this study, the MNDWI index values vary from - 0.7 to 0.2 in the particular period. The spatial variability of index values varies evidently with the variation of years. The decline of vegetation area and increase in water area is also clearly discernible over the years (Fig. 6; Table 3). The images were classified into five classes based on MNDWI index values: wet-land, shallow water, bare land, green vegetation and moderate green vegetation. The shallow water area (mostly covered with rivers) was 726 km^2 in 1989, enlarged to 1271 km^2 in 2000, in 2014 declined to 660 km^2, and in 2020 further declined to 397 km^2. Finally, from 1989 to 2020, the shallow water area decreased by $^{\sim}$14.30 km^2 yr^{-1} (Fig. 7). The wet-land area (mostly covered with *beels* and water logging areas) was 201 km^2 in 1989, enlarged to 358 km^2 in 2000, in 2014 further enlarged to 1244 km^2, and in 2020 more enlarged to 2415 km^2. In conclusion, from 1989 to 2020, the wet-land area enlarged by $^{\sim}$ 67.12 km^2 yr^{-1} (Fig. 7). The bare land area also enlarged to a rate of $^{\sim}$

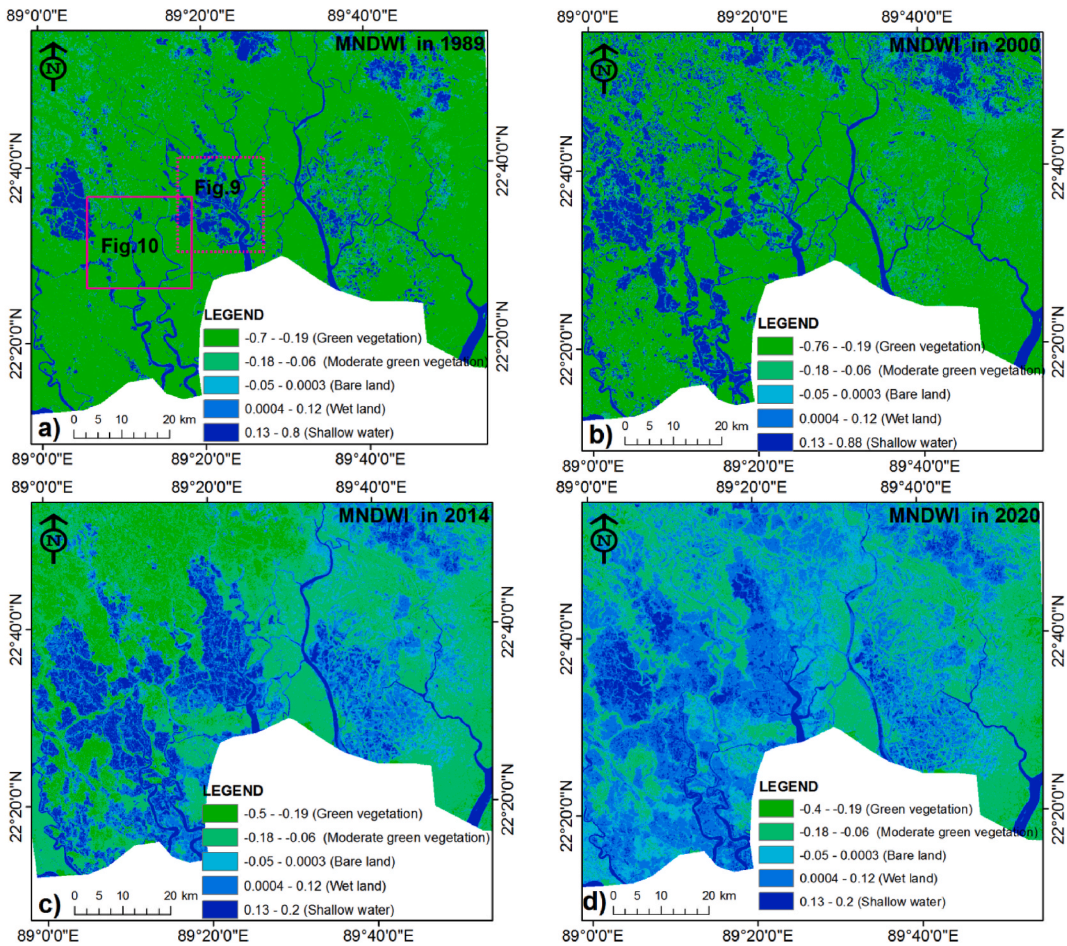

Fig. 6. Spatial distribution of MNDWI for 1989, 2000, 2014, and 2020.

Table 2
MNDWI classification and accuracy assessment analysis.

Year	User accuracy (%)					Producer accuracy (%)					Overall accuracy (%)	Kapa Coefficient
	Shallow water	Wet land	Bare land	Moderate green vegetation	Green vegetation	Shallow Water	Wet land	Bare land	Moderate green vegetation	Green vegetation		
1989	90	83.3	62.5	66.7	70.0	90	71.4	71.4	50	87.5	75.0	68.6
2000	100	100	75	50.0	54.6	100	84.6	60	50	75.0	77.5	71.2
2014	90.9	80	70	71.4	85.7	100	80	87.5	55.6	75.0	80.0	74.72
2020	100	100	62.5	50.0	83.3	100	85.7	83.3	50	71.4	82.5	77.4

Table 3
MNDWI classification results in different times (km^2).

	Shallow water	Wet land	Bare land	Moderate green vegetation	Green vegetation
1989	726	201	163	565	5118
2000	1271	358	235	811	4096
2014	660	1244	768	2761	1233
2020	397	2415	1457	2256	138

39.36 km^2 yr^{-1}. The moderate green vegetation area was 565 km^2 in 1989, increased to 811 km^2 in 2000, in 2014 further increased to 2761 km^2, and in 2020 again decreased to 2256 km^2. Finally, from 1989 to 2020, the moderate green vegetation area enlarged by ~ 69.77 km^2 yr^{-1} (Fig. 7). However, the green vegetation area decreased at a rate of ~166.1 km^2 yr^{-1}.

4. Discussion

The study reveals that from 1989 to 2020, the shallow water area (mostly covered with rivers) decreased by ~ 14.30 km^2 yr^{-1}, whereas the wet-land area (mostly covered with beels and waterlogging areas) increased by ~ 67.12 km^2 yr^{-1} (Figs. 6–7; Table 3). The bare land area also increased at a rate of ~ 36.90 km^2 yr^{-1}. Conversely, the green vegetation area decreased at a rate of ~ 166.1 km^2 yr^{-1}, whereas the moderate green vegetation area increased by ~ 69.77 km^2 yr^{-1} for the same period. The positive value of MNDWI indicates water content, and the positive value increases which reflects more water content or more water depths [30,53]. However, the MNDWI analysis reflects that the positive values gradually decreased reflecting the decrease in water depth ([30,53]; Fig. 6).

The GBM rivers system is the mainstay of lowland water discharge and stability of the lowland biodiversity of the Bengal basin. These initiate in the Himalayas and transmit the expected yearly sediment of ~500 million tons to ~1.4 billion tons [65–67]; Fig. 3d], discharge ~1.5 million m^3 s^{-1} during peak periods [68], and have a strong effect on the lowlands through sedimentation, though sedimentation is gradually decreasing in the delta (Fig. 3d) from the upstream due to anthropogenic activities [19,43,51]. In the Indian

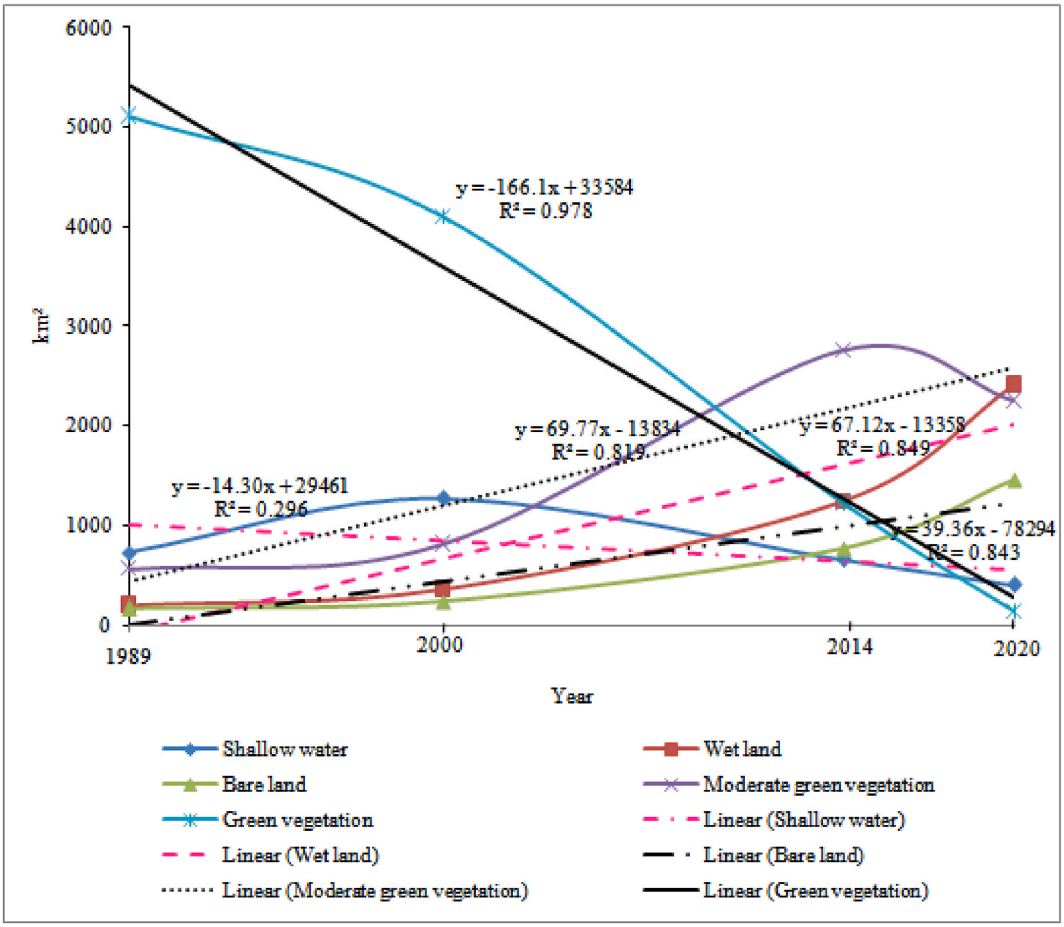

Fig. 7. MNDWI classification results from 1989 to 2020 and trend lines.

subcontinent, southwesterly winds blow from the BoB to the coast from June to September, causing continuous rainfall (Fig. 3b and c) and flooding all through the area. Barua et al. [69] found that in the BoB, the way of residual current and sedimentation is landward and westward. As a consequence, nearby tides and waves affect the internal turbulent water through a concentrated association of tidal channels, and distribute sediment across the low tide deltaic plain [44]. However, in the coastal areas of Bangladesh, especially on the SW coast, more sedimentation is going on within the channels (Fig. 2a,e) rather than in the fluvio-tidal and tidal plains due to the combined effects of polders, embankments and upstream barrages [12,19,70].

Embankments and polders were assembled in the coastal zones of Bangladesh to shield the areas from salt-water imposition. But these also stop sedimentation of tidal lowlands [12,13,19,71], and sedimentation taking place within the channels rather than plain lands. In addition, due to the upstream dam [72], the distributaries of the Ganges release very little water in the SW coastal parts of Bangladesh, particularly during the dry period (Fig. 8) when precipitation also low in the region (Fig. 2a–c), resulting in more tidal sedimentation within the channels, as the upstream water power is very low in contrast with the flood tides. Islam and Gnauck, Goodbred and Kuehl [73,74] stated that due to the Farakka Barrage in India since 1975, the discharge of the Ganges reduced to 370 $m^3 s^{-1}$ in 2010 from 3700 $m^3 s^{-1}$ in 1962. So, due to the combined result of dams, polders, and upstream shortages of discharge during the dry season, supplementary sedimentation is taking place within the channels instead of in the adjacent plain lands. Consequently, channels are regularly silted (due to siltation, depths gradually decreased), congested, and many cases abandoned ([11–13,19]; Fig. 2a, e; Figs. 9 and 10). Therefore, tidal channels are raising their beds due to excessive sedimentation, and are also obscuring drains from polder lands [12,19,20,41,75]. Therefore, the shallow water area (mostly covered by rivers) and its depths are gradually decreasing, which is also exposed through MNDWI analysis (Figs. 6, 9 and 10). On the other hand, the tidal plains areas are gradually going below sea level due to a deficit of sedimentation and compaction of loose coastal sediments [12,19]. Consequently, during channel movement or storm surges, the landscape is unwrapped up for tidal flooding and waterlogging [12], reasoning salinization of the area [47,75]. Moreover, the BoB is a well-known ground for tropical cyclones. However, recently its frequency is increasing due to climate change [8], and consequently more waterlogging and more suffering as shallow low lands (Fig. 2b,c,e). Auerbach et al. [20] documented that due to the deficit of sedimentation, polder lands are now located about 1 m below the mean high-water level. As a result, the wet-land area (mostly covered with *beels* and water logging areas) is gradually increasing. Due to the increase of wet-land, the people now convert their agricultural land to the saline water dependent fish firm [63]. Therefore, salinity is increasing both in surface and subsurface water, and also in the soils, and these are affecting the natural biodiversity [9,20,41,76–80]. Rashid et al. and Alongi [8,9, 81] stated that the SW coastal region of Bangladesh is extremely susceptible to a decline in freshwater, salinity intrusion and climate change. The saline situation affects the growth of trees and crops through prying with nutrient uptake, dropping intensification, and stopping plant reproduction. Salinity is also connected to wetness and deficit of surface cover and thus increases the disclosure of soils to erosion. Therefore, the agriculture and vegetation in the areas are severely affected. Therefore, the green vegetation severely decreased in the area, and the bare land area increased.

To attain the Sustainable Development Goals (SDGs) by 2030, the United Nations Development Programme (UNDP) received 17 international goals. These cover social and economic growth matters including education, hunger, poverty, gender equality, health, urbanization, social justice, sanitation, water, energy, environment, and global warming [82]. Of the 17 Goals, the Goal 13 is intended for Climate action. Due to climate alteration, heatwaves, droughts and floods occur frequently which are destroying the earth and distressing billions of lives worldwide. Therefore, increasing climate events and succession toward an insistent change is indispensable for reducing the climate threats and taking the priorities for sustainable growth, including human safety, water, food, and so on. Climate alterations not only impact the country's economics but also the livelihoods and lives, predominantly those who are in vulnerable conditions [83] like Bangladesh. It also leads to spreading global cropland dilapidation, and thus poverty [84]. The SDG-6 is

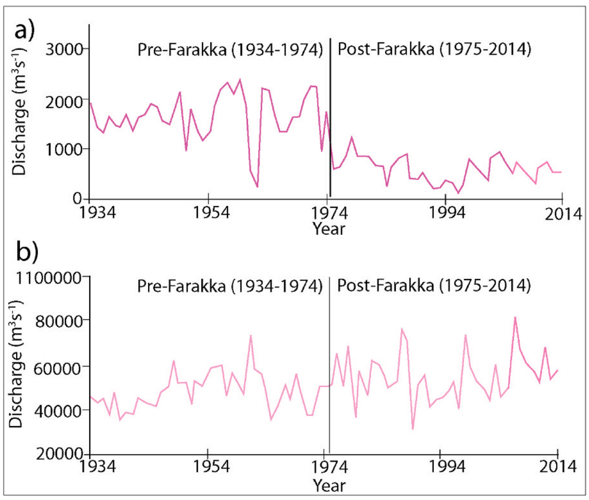

Fig. 8. Pre- and post Farakka period water discharge of Ganges (Padma) River at Hardinge Bridge Pakshi, Pabna, Bangladesh (Source: Bangladesh Water Development Board (BWDB)).

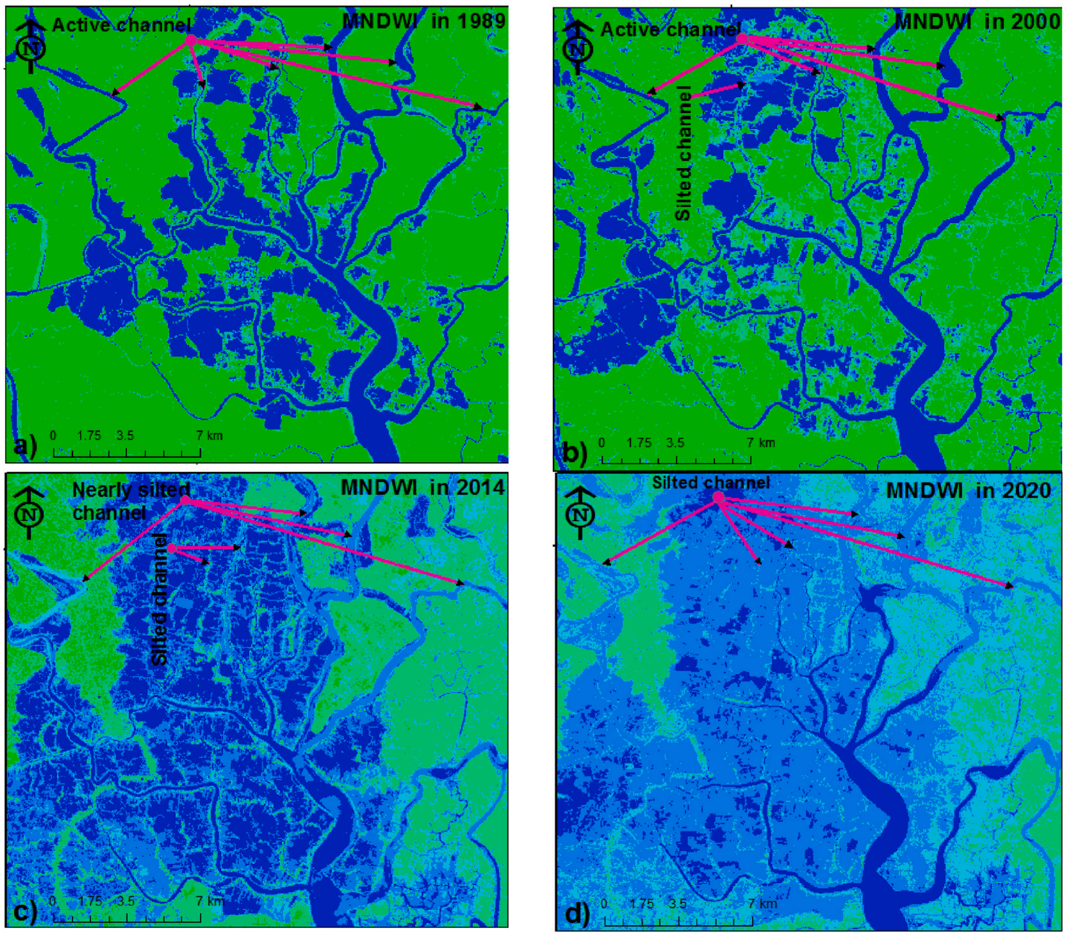

Fig. 9. The area-wise expansion of the drainage map and waterlogging area (Please see Fig. 6a for location of the area, and see Fig. 6a–d for legend of Fig. 9a–d, respectively).

intended for Clean Water and Sanitation to guarantee convenience and sustainable running of water for everyone especially, paying special attention to those in vulnerable states like the SW coastal area of Bangladesh. To accomplish the goal, expand global collaboration, and capacity-building carry to developing states in water-related plans and activities, counting wastewater treatment, desalination, water harvesting, water efficiency, reuse and recycling technologies were included. Access to safe water is the most basic human requirement for well-being and health.

The relative sea level increase in the Bangladesh coast is ~1–9 mm yr^{-1} [75,85–88] and the average sedimentation rate is ~ 2.12–4.59 mm yr^{-1} [19,47]. Due to the rise of the sea level of 1 m by 2050, Bangladesh could lose 17% of its land [89], and consequently, 20 million people will become refugees [90,91]. The GBM delta is one of the biggest deltas in the earth including 100, 000 km^2 of deltaic plains, riverine floodplains, and coastal plains with rich biodiversity [92]. Over the last three decades, globally, the threat of species annihilation has deteriorated by ~10% [93]. SDG-15 is for Life on Land, and it is adopted to restore, protect, and encourage sustainable utilization of worldwide ecosystems, prevent desertification, sustainably handle forests, and halt and upend land deprivation and prevent biodiversity loss. Approximately 30% of the earth's surface is wrapped by vegetation which supplies vital habitats for millions of species. It is the leading natural source of freshwater and air and is being considered as an indispensable constituent for combating the alters in the climate [94]. Thus, for sustainable growth, efficient action includes not only hastening the pace of alter but also appropriate addressing of the behind vulnerability drivers and allowing the stakeholders, diverse communities, sectors, regions, and cultures to join in just, equitable, and inclusive procedures that develops in general health and welfare of the people in the planet. However, due to the effect of both natural (sea level rise, climate change, storm surges, and cyclones, etc.) and anthropogenic (polders, embankments, upstream dams, etc.), processes, and consequently land subsidence [19], waterlogging and flooding [12], salinity increase [9,76], coastal erosion [95–97], etc., made the coastal areas of Bangladesh in a vulnerable situation both for humans and natural biodiversity. The outputs of the research will be helpful for planners, policy makers, coastal scientists all over the sphere, etc. To understand the reality of the SW coastal parts of the country, and in conclusion sustainable running of the vital coastal ecosystem.

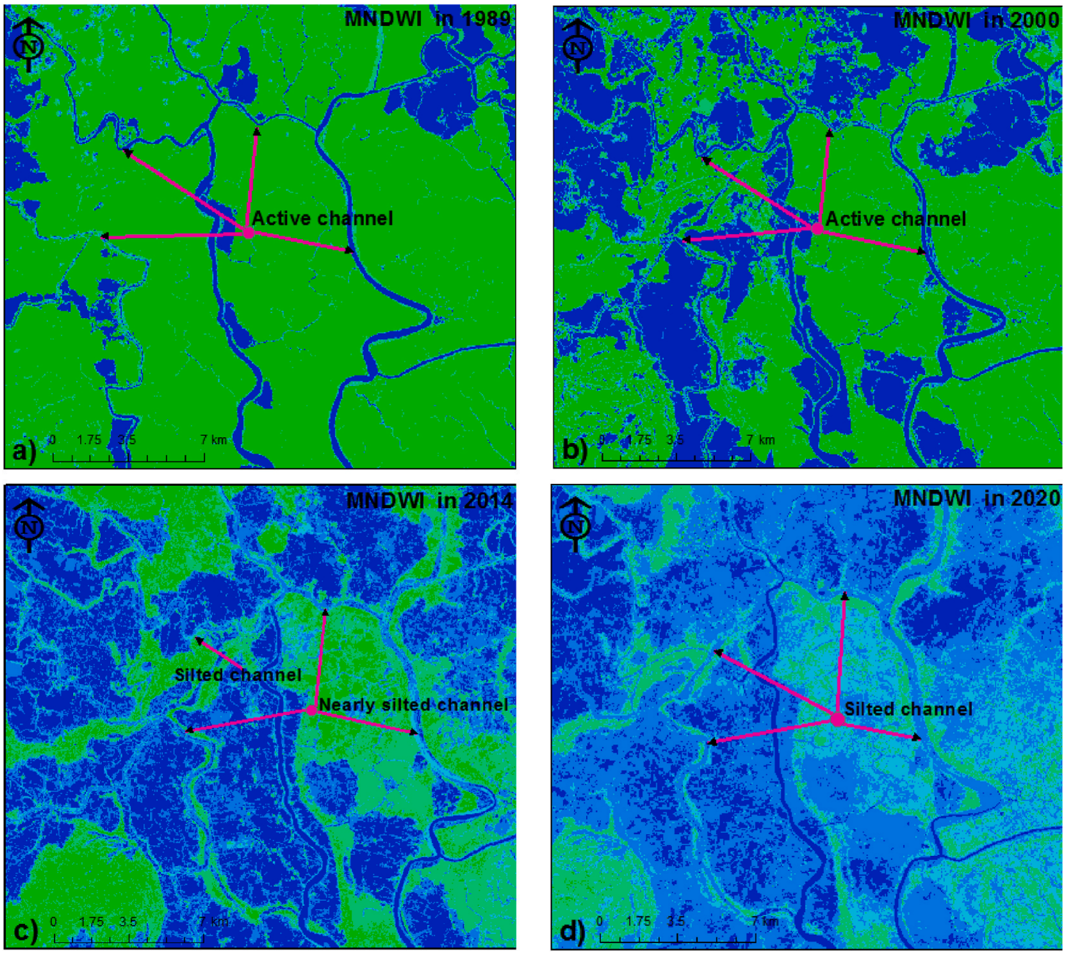

Fig. 10. The area-wise expansion of the drainage map and waterlogging area (Please see Fig. 6a for location of the area, and see Fig. 6a–d for legend of Fig. 10a–d, respectively).

5. Conclusion

This research used satellite image analysis and GIS to identify and examine the spatial changes and quantify the waterlogging areas and drainage system change of the SW coastal part of Bangladesh. Using satellite images to identify information concerning waterlogging area and drainage system change is quicker and more precise than other examination methods, particularly in delineating changes between two or more dissimilar time intervals. The MNDWI analysis clearly exposed the vulnerable situation of the SW coastal parts of Bangladesh due to the anthropogenic and natural processes. The rivers area and their depths are gradually declining, whereas the waterlogging and bare land areas are increasing. The green vegetation areas are decreasing due to waterlogging and salinity increase. The output of the study will be useful for coastal scientists worldwide, policy makers, planners, etc., and will also be valuable for the potential sustainable management of the crucial coastal ecosystem including the GB delta coast.

Finally, the following recommendations should be taken to defend the drainage congestion, water logging, and finally sustainable management of the area: (1) make sure tidal creeks and channels operate as an inlets and outlets of tidal plain areas, (2) ensure sufficient water discharge from upstream to the delta plains in the dry season (3) prior study is required including coastal scientists, engineers, policymakers, planners, etc., for any sort of polder, embankments and dam construction.

Author contribution statement

Md. Bazlar Rashid: Conceived and designed the experiments; Performed the experiments; Analyzed and interpreted the data; Contributed reagents, materials, analysis tools or data; Wrote the paper.

Funding statement

This research did not receive any specific grant from funding agencies in the public, commercial, or not-for-profit sectors.

Data availability statement

Data will be made available on request.

Declaration of competing interest

The authors declare that they have no known competing financial interests or personal relationships that could have appeared to influence the work reported in this paper.

Acknowledgements

The authors would like to convey their cordial thanks and deep gratitude to Mohammad Elius Hossain, Director General, Geological Survey of Bangladesh (GSB) for giving the chance to carry out the work. The authors also convey their thanks to the USGS authority for permission to utilize satellite images. We would also like to pay our special thanks to Dr. Rahat Khan, Bangladesh Atomic Energy Commission, Mr. Felix Frimpong CSIR-Crops Research Institute Research Scientist (Climate Change resilience) P. O. Box 3785 Fumesua, Kumasi, Ghana for their help in proofing the manuscript.

References

[1] M. Elhag, Evaluation of different soil salinity mapping using remote sensing techniques in arid ecosystems, Saudi Arabia. J. Sens. (2016), 7596175.
[2] T.B. Ramos, H. Darouich, J. Šimůnek, M.C. Goncalves, J.C. Martins, Soil salinization in very high-density olive orchards grown in southern Portugal: current risks and possible trends, Agric. Water Manag. 217 (2019) 265–281.
[3] H. Nouri, S.C. Borujeni, S. Alaghmand, S.J. Anderson, P.C. Sutton, S. Parvazian, S. Beecham, Soil salinity mapping of urban greenery using remote sensing andproximal sensing techniques; the case of veale gardens within the Adelaide parklands, Sustainability 10 (8) (2018) 2826.
[4] H.T. Fourati, M. Bouaziz, M. Benzina, S. Bouaziz, Detection of terrain indices related to soil salinity and mapping salt-affected soils using remote sensing and geostatistical techniques, Environ. Monit. Assess. 189 (2017) 177.
[5] Y. Rongjiang, Y. Jingsong, Quantitative evaluation of soil salinity and its spatial distribution using electromagnetic induction method, Agric. Water Manag. 97 (2010) 1961–1970.
[6] K.A. Nguyen, Y.A. Liou, H.P. Tran, P.P. Hoang, T.H. Nguyen, Soil salinity assessment by using nearinfrared channel and vegetation soil salinity index derived from landsat 8 OLI data: a case study in the tra vinh province, mekong delta, vietnam, Prog. Earth Planet. Sci. 7 (2020) 1.
[7] A. Nishat, Review of present activities and state of art of the coastal areas of Bangladesh, in: *Coastal Area Resource Development And Management*. Part II, Coastal Area Resource Development and Management Association (CARDMA), Dhaka, Bangladesh, 1988, pp. 23–35.
[8] M.B. Rashid, M.R. Sheikh, A.J.M.E. Haque, M.A.A. Patwary, Climate change impact and frequency of cyclone surge in Bangladesh coast: proper plan to address sustainably, Int. J. Econ. Environ. Geol. 13 (2) (2022) 15–20.
[9] M.B. Rashid, M.R. Sheik, A.J.M.E. Haque, M.A.B. Siddique, M.A. Habib, M.A.A. Patwary, Salinity-induced change in green vegetation and land use patterns using remote sensing, NDVI, and GIS techniques: a case study on the southwestern coast of Bangladesh, Case Stud. Chem. Environ. Eng. (2023), 100314, https://doi.org/10.1016/j.cscee.2023.100314.
[10] A. Nishat, Disaster and Climate Resilience: Bangladesh Perspectives, International Conference on Earth and Environmental Sciences and Technology, 2020, p. 19. https://iceest.info./.
[11] C.A. Wilson, S.L. Goodbred Jr., C. Small, J. Gilligan, S. Sams, B. Mallick, R. Hale, Widespread infilling of tidal channels and navigable waterways in human-modified tidal deltaplain of southwest Bangladesh, Elementa 5 (2017) 78, https://doi.org/10.1525/elementa.263.
[12] M.B. Rashid, A. Mahmud, M.K. Ahsan, M.H. Khasru, M.A. Islam, Drainage congestion and its impact on environment in the south-western coastal part of Bangladesh, Bangladesh J. Geol. 31 (32) (2013) 43–55.
[13] M.B. Rashid, M. Hasan, A. Mahmud, Adverse impact on drainage system by unplanned human intervention in the south-western coastal part of Bangladesh, Book of Abstracts, ISBN: 978-85-64964-09-9, in: Ninth International Conference on Coastal and Port Engineering in Developing Countries (PIANC-COPEDEC IX), Rio De Jeneiro, Brazil, 2016, pp. 90–91, www.pianc-copedec2016.com.
[14] K. Ahsan, M.B. Rashid, S. Talukder, Tidal River siltation and its impact in the coastal parts of Bangladesh, Int. J. Econ. Environ. Geol. 13 (2) (2022) 35–41.
[15] W.B. Bull, The alluvial fan environment, Prog. Phys. Geogr. 1 (1977) 222–270.
[16] M.B. Rashid, Channel bar development and bankline migration of the Lower Padma River of Bangladesh, Arabian J. Geosci. 13 (2020) 612, https://doi.org/10.1007/s12517-020-05628-9.
[17] M.B. Rashid, M.A. Habib, R. Khan, A.R.M.T. Islam, Land transform and its consequences due to the route change of the Brahmaputra River in Bangladesh, Int. J. River Basin Manag. (2021), https://doi.org/10.1080/15715124.2021.1938095.
[18] M.B. Rashid, M.A. Habib, Channel bar development, braiding and bankline migration of the Brahmaputra-Jamuna River, Bangladesh through RS and GIS techniques, Int. J. River Basin Manag. (2022), https://doi.org/10.1080/15715124.2022.211828.
[19] M.B. Rashid, K. Ahsan, A.B.K. Majlis, M.K. Ahsan, A. Mahmud, Sedimentation and coastal area management in the human-modified Ganges-Brahmaputra tidal delta plain of Bangladesh, Int. J. River Basin Manag. (2022) 1–13, https://doi.org/10.1080/15715124.2022.2092489.
[20] L.W. Auerbach, S.L. Goodbred Jr., D.R. Mondal, C.A. Wilson, K.R. Ahmed, K. Roy, et al., Reply to Tidal river management in Bangladesh, Nat. Clim. Change 5 (2015) 492, https://doi.org/10.1038/nclimate2472.
[21] Y.O. Ouma, R. Tateishi, A water index for rapid mapping of shoreline changes of five East African Rift Valley lakes: an empirical analysis using Landsat TM and ETM+ data, Int. J. Rem. Sens. 27 (2006) 3153–3181.
[22] C. Giardino, M. Bresciani, P. Villa, A. Martinelli, Application of remote sensing in water resource management: the case study of Lake Trasimeno, Italy, Water Resour. Manag. 24 (2010) 3885–3899.
[23] V.M. Chowdary, R.V. Chandran, N. Neeti, R.V. Bothale, Y.K. Srivastava, P. Ingle, D. Ramakrishnan, D. Dutta, A. Jeyaram, J.R. Sharma, et al., Assessment of surface and sub-surface waterlogged areas in irrigation command areas of Bihar state using remote sensing and GIS, Agric. Water Manag. 95 (2008) 754–766.
[24] M.M. Taghadosi, M. Hasanlou, K. Eftekhari, Retrieval of soil salinity from Sentinel-2 multispectral imagery, Eur. J. Remote Sens. 52 (1) (2019) 138–154.
[25] K.N.P. Raju, M.K. Pandey, S. Sarkar, A note on boundaries in atlas maps, J. Geol. Soc. India 83 (2014) 563–566.
[26] B. Guo, F. Yang, B. Han, Y. Fan, L. Jiang, A model for the rapid monitoring of soil salinization in the yellow river delta using landsat 8 OLI imagery based on VI-SI feature space, Remote Sens. Lett. 10 (2019) 796–805.
[27] J. Wang, J. Peng, H. Li, C. Yin, W. Liu, T. Wang, H. Zhang, Soil salinity mapping using machine learning algorithms with the sentinel-2 MSI in arid areas, China, Rem. Sens. 13 (2021) 305.
[28] H. Frey, C. Huggel, F. Paul, W. Haeberli, Automated detection of glacier lakes based on remote sensing in view of assessing associated hazard potentials Grazer Schriften Geogr, Raumforsch 45 (2010) 261–272.
[29] J.W. Rouse, R.H. Haas, J.A. Schell, D.W. Deering, Monitoring vegetation systems in the great plains with ERTS, Third 80 ERTS Symposium 351 (1973) 309–317. NASA SP.

[30] H. Xu, Modification of normalized difference water index (NDWI) to enhance open water features in remotely sensed imagery, Int. J. Rem. Sens. 27 (14) (2006) 3025–3033.
[31] Z. Duan, W.G.M. Bastiaanssen, Estimating water volume variations in lakes and reservoirs from four operational satellite altimetry databases and satellite imagery data, Remote Sens. Environ. 134 (2013) 403–416.
[32] G.L. Feyisa, H. Meilby, R. Fensholt, S.R. Proud, Automated Water Extraction Index: a new technique for surface water mapping using Landsat imagery, Remote Sens. Environ. 140 (2014) 23–35.
[33] A. Davranche, G. Lefebvre, B. Poulin, Wetland monitoring using classification trees and SPOT-5 seasonal time series, Remote Sens. Environ. 114 (2010) 552–562.
[34] B. Poulin, A. Davranche, G. Lefebvre, Ecological assessment of Phragmites australis wetlands using multi-season SPOT-5 scenes, Remote Sens. Environ. 114 (2010) 1602–1609.
[35] L. Ji, L. Zhang, B. Wylie, Analysis of dynamic thresholds for the normalized difference water index, Photogramm. Eng. Rem. Sens. 7 (2009) 1307–1317.
[36] S. Lu, B. Wu, N. Yan, H. Wang, Water body mapping method with HJ-1A/B satellite imagery, Int. J. Appl. Earth Obs. Geoinf. 13 (2011) 428–434.
[37] K.V. Singh, R. Setia, S. Sahoo, A. Prasad, B. Pateriya, Evaluation of NDWI and MNDWI for assessment of waterlogging by integrating digital elevation model and ground water level, Geocarto Int. 30 (6) (2015) 650–661, https://doi.org/10.1080/10106049.2014.965757.
[38] S. Paul, S. Pal, Predicting wetland area and water depth of Ganges moribund deltaic parts of India, Remote Sens. Appl.: Soc. Environ. 19 (2020), 100338, https://doi.org/10.1016/j.rsase.2020.100338.
[39] I. Orimoloye, S. Mazinyo, W. Nel, A. Kalumba, Spatiotemporal monitoring of land surface temperature and estimated radiation using remote sensing: human health implications for East London, South Africa, Environ. Earth Sci. 77 (3) (2018) 1–10.
[40] I.R. Orimoloye, A.M. Kalumba, S.P. Mazinyo, W. Nel, Geospatial analysis of wetland dynamics: wetland depletion and biodiversity conservation of Isimangaliso Wetland, J. King Saud Univ. Sci. 32 (2020) 90–96.
[41] L.W. Auerbach, S.L. Goodbred Jr., D.R. Mondal, C.A. Wilson, K.R. Ahmed, K. Roy, et al., Flood risk of natural and embanked landscapes on the Ganges-Brahmaputra tidal delta plain, Nat. Clim. Change 5 (2015) 153–157, https://doi.org/10.1038/nclimate2472.
[42] A.K. Gain, D. Benson, R. Rahman, D.K. Datta, J.J. Rouillard, Tidal river management in the south west Ganges-Brahmaputra delta in Bangladesh: moving towards a transdisciplinary approach? Environ. Sci. Pol. 75 (2017) 111–120.
[43] F.E. Dunn, R.J. Nicholls, S.E. Darby, S. Cohen, C. Zarfl, M. Balázs, B.M. Fekete, Projections of historical and 21st century fluvial sediment delivery to the Ganges-Brahmaputra-Meghna, Mahanadi, and Volta deltas, Sci. Total Environ. 642 (2018) 105–116, https://doi.org/10.1016/j.scitotenv.2018.06.006.
[44] R.P. Hale, R. Bain, S.L. Goodbred Jr., J. Best, Observations and scaling of tidal mass transport across the lower Ganges-Brahmaputra delta plain: implications for delta management and sustainability, Earth Surf. Dyn. 7 (2019) 231–245, https://doi.org/10.5194/esurf-2018-66.
[45] E.J. Bomer, C.A. Wilson, R.P. Hale, A.N.M. Hossain, F.M.A. Rahman, Surface elevation and sedimentation dynamics in the Ganges-Brahmaputra tidal delta plain, Bangladesh: evidence for mangrove adaptation to human induced tidal amplification, Catena 187 (2020), 104312.
[46] M.M. Rahman, A. Haque, R.J. Nicholls, S.E. Darby, M.T. Urmi, M.M. Dustegir, F.E. Dunn, A. Tahsin, S. Razzaque, K. Horsburg, M.A. Haque, Sustainability of the coastal zone of the Ganges-Brahmaputra-Meghna delta under climatic and anthropogenic stresses, Sci. Total Environ. 829 (2022), 54547, https://doi.org/10.1016/j.scitotenv.2022.154547.
[47] M.B. Rashid, M.A. Habib, A. Mahmud, M.K. Ahsan, M.H. Khasru, M.A. Hossain, A. Ahsan, K.M. Akther, S. Talukder, Tectonic Setting, Provenance, Depositional, and Paleo-Climatic Conditions of the Late Quaternary Subcrop Sediments of the Southeastern Coastal Region of the Bengal Basin, Heliyon, 2023, e12998, https://doi.org/10.1016/j.heliyon.2023.e12998. ISSN 2405-8440.
[48] M.B. Rashid, A. Mahmud, M.K. Ahsan, M.H. Khasru, K. Ahsan, M.A. Habib, M.A. Hossain, M.F. Alam, Role of major rivers for the development of ganges-brahmaputra delta, Int. J. Econ. Environ. Geol. 5 (1) (2014) 25–32, https://doi.org/10.46660/ijeeg.Vol0.Iss0.0.108.
[49] D.G. Zawada, J.C. Brock, A multiscale analysis of coral reef topographic complexity using lidar-derived bathymetry, J. Coast Res. (SI) (2009) 6–15.
[50] V. Chirayath, S.A. Earle, Drones that see through waves-Preliminary results from airborne fluid lensing for centimetre-scale aquatic conservation, Aquat. Conserv. Mar. Freshw. Ecosyst. 26 (S2) (2016) 237–250.
[51] S.J. Purkis, Remote sensing tropical coral reefs: the view from above, Ann. Rev. Mar. Sci 10 (1) (2018) 149–168.
[52] J.M. Kerr, S. Purkis, An algorithm for optically-deriving water depth from multispectral imagery in coral reef landscapes in the absence of ground-truth data, Remote Sens. Environ. 210 (2018) 307–324.
[53] H. Xu, A study on information extraction of water body with the modified normalized difference water index (MNDWI), J. Remote Sens. 9 (2005) 589–595.
[54] E.C. Geyman, A.C. Maloof, A simple method for extracting water depth from multispectral satellite imagery in regions of variable bottom type, Earth Space Sci. (2019) 6527–6537, https://doi.org/10.1029/2018EA000539.
[55] M. Mahdianpari, B. Salehi, F. Mohammadimanesh, M. Motagh, Random forest wetland classification using ALOS-2 L-band, RADARSAT-2 C-band, and TerraSAR-X imagery, ISPRS J. Photogrammetry Remote Sens. 130 (2017) 13–31.
[56] C. Lo, J. Choi, A hybrid approach to urban land use/cover mapping using Landsat 7 Enhanced Thematic Mapper Plus (ETM+) images, Int. J. Rem. Sens. 25 (2004) 2687–2700.
[57] K. Rokniet, A. Ahmad, A. Selamat, S. Hazini, Water feature extraction and change detection using Multitemporal Landsat Imagery, Rem. Sens. 6 (2014) 4173–4189, https://doi.org/10.3390/rs6054173.
[58] M.M. Rahman, M. Ullah, M. Lan, J.T. Sumantyo, H. Kuze, R. Tateishi, Comparison of Landsat image classification methods for detecting mangrove forests in Sundarbans, Int. J. Rem. Sens. 34 (2013) 1041–1056.
[59] W.A.D.B. Weerasingha, A.S. Ratnayake, Coastal landform changes on the east coast of Sri Lanka using remote sensing and geographic information system (GIS) techniques, Remote Sens. Appl.: Soc. Environ. 26 (2022), 100763, https://doi.org/10.1016/j.rsase.2022.100763.
[60] A.K.M.K. Alam, M.B. Islam, Recent changes in Jadukata fan (Bangladesh) in response to Holocene tectonics, Quat. Int. 462 (2017) 226–235, https://doi.org/10.1016/j.quaint.2017.08.014.
[61] P.P. Adhikary, D. Barman, M. Madhu, et al., Land use and land cover dynamics with special emphasis on shifting cultivation in Eastern Ghats Highlands of India using remote sensing data and GIS, Environ. Monit. Assess. 191 (2019) 315, https://doi.org/10.1007/s10661-019-7447-7.
[62] N.J. Kraff, M. Wurm, H. Taubenböck, Uncertainties of human perception in visual image interpretation in complex urban environments, IEEE J. Sel. Top. Appl. Earth Obs. Rem. Sens. 13 (2020) 4229–4241.
[63] M.J. Faruque, Z. Vekerdy, M.Y. Hasan, K.J. Islam, B. Young, M.T. Ahmed, M.U. Monir, S.M. Shovon, J.F. Kakon, P. Kundu, Monitoring of land use and land cover changes by using remote sensing and GIS techniques at human-induced mangrove forests areas in Bangladesh, Remote Sens. Appl.: Soc. Environ. 25 (2022), 100699, https://doi.org/10.1016/j.rsase.2022.100699. ISSN 2352-9385.
[64] V.K. Gautam, P.K. Gaurav, P. Murugan, M. Annadurai, Assessment of surface water dynamicsin Bangalore using WRI, NDWI, MNDWI, supervised classification and K-T transformation, Aqua. Proc. 4 (2015) 739–746, https://doi.org/10.1016/j.aqpro.2015.02.095.
[65] K.M. Elahi, S.C. Das, S. Sultana, Geography of coastal environment: a study of selected issues, in: A. Bayes, A. Muhammad (Eds.), An Analytical Discourse on Development, The University Press Limited, Dhaka, 1998, pp. 336–368.
[66] H.R. Kudrass, K.H. Michels, M. Wiedicke, A. Suckow, Cyclones and tides as feeders of a submarine canyon of Bangladesh, Geology 26 (1998) 715–718.
[67] M.M. Rahman, M. Dustegir, R. Karim, A. Haque, R.J. Nicholls, S.E. Darby, H. Nakagawa, M. Hossain, F.E. Dunn, M.M. Akter, Recent sediment flux to the Ganges-Brahmaputra-Meghna delta system, Sci. Total Environ. 643 (2018) 1054–1064, https://doi.org/10.1016/j.scitotenv.2018.06.147.
[68] S. Hasan, G. Mulamoottil, Natural resource management in Bangladesh, Ambio 23 (1994).
[69] D.K. Barua, S.A. Kuehl, R.L. Miller, W.S. Moore, Suspended sediment distribution and residual transport in the coastal ocean off the Ganges-Brahmaputra river mouth, Mar. Geol. 120 (1994) 41–61, https://doi.org/10.1016/0025-3227(94)90076-0.
[70] S. Samanta, S. Hazra, P.P. Mondal, A. Chanda, S. Giri, J.R. French, R.J. Nicholls, Assessment and attribution of mangrove forest changes in the Indian sundarbans from 2000 to 2020, Rem. Sens. 13 (2021) 4957, https://doi.org/10.3390/rs13244957.

[71] K.G. Rogers, Jr.S.L. Goodbred, D.R. Mondal, Monsoon sedimentation on the 'abandoned' tide-influenced Ganges-Brahmaputra delta plain, Estuar. Coast Shelf Sci. 131 (2013) 297–309, https://doi.org/10.1016/j.ecss.2013.07.014.
[72] A.R.M.T. Islam, S. Talukdar, S. Akhter, K.U. Eibek, M.M. Rahman, S. Pal, M.W. Naikoo, A. Rahman, A. Mosavi, Assessing the impact of the Farakka barrage on hydrological alteration in the Padma River with future insight, Sustainability 14 (2022) 5233, https://doi.org/10.3390/su14095233.
[73] S.N. Islam, A. Gnauck, Threats to the Sundarbans mangrove wetland ecosystems from transboundary water allocation in the Ganges basin: a preliminary problem analysis, Int. J. Ecol. Econ. Stat. 13 (2009) 64–78.
[74] S.L. Goodbred Jr., S.A. Kuehl, The significance of large sediment supply,active tectonism, and eustasy on margin sequence development; Late Quaternary stratigraphy and evolution of theGanges-Brahmaputra delta, Sediment. Geol. 133 (2000) 227–248.
[75] J. Pethick, J.D. Orford, Rapid rise in effective sea-level in southwest Bangladesh: its causes and contemporary rates, Global Planet. Change 111 (2013) 237–245, https://doi.org/10.1016/j.gloplacha.2013.09.019.
[76] M.A.B. Siddique, R. Khan, A.R.M.T. Islam, M.K. Alam, M.S. Islam, M.S. Hossain, M.A. Habib, M.A. Akbor, U.H. Bithi, M.B. Rashid, M. Hossain, I.M.M. Rahman, I. B. Elius, M.S. Islam, Quality assessment of freshwaters from a coastal city of southern Bangladesh: irrigation feasibility and preliminary health risks appraisal, Environ. Nanotechnol. Monit. Manag. 16 (2021), https://doi.org/10.1016/j.enmm.2021.100524.
[77] W.M. Ullah, R. Rahman, Tidal River management, in: BAPA (Ed.), A Sustainable Solution to Drainage Congestion in the Coastal Region vol. 2, Bangladesh Environment, Dhaka, 2002, pp. 1022–1032.
[78] A.A. Tutu, River Management in Bangladesh: a People's Initiative to Solve Water-Logging, vol. 52, International Institute for Environment and Development (IIED), London, 2005, pp. 117–123.
[79] A. Paul, B. Nath, M.R. Abbas, Tidal River Management (TRM) and its implication in disaster management: a geospatial study on Hari-Teka river basin, Jessore, Bangladesh, Int. J. Geomatics Geosci. 4 (1) (2013) 125–135.
[80] M.M.A. Masud, N.N. Moni, A.K. Azad, Impacts of water logging on biodiversity - study on south-western region of Bangladesh, IOSR J. Environ. Sci. Toxicol. Food Technol. 8 (2014) 20–27. www.iosrjournals.org.
[81] D.M. Alongi, Present state and future of the world's mangrove forests, Environ. Conserv. 29 (3) (2002) 331–349.
[82] Anon, Press release - UN general assembly's open working group proposes sustainable development goals" (PDF), Sustainabledevelopment.un.org 2014 (2014), 19 July. (Accessed 18 October 2016).
[83] Anon, Goal 13: Climate Action, Archived from the Original on 13 August 2018, UNDP, 2018. Retrieved on (Accessed 12 March 2018).
[84] Anon, Desertification, land degradation and drought sustainable development knowledge platform, Sustainabledevelopment.un.org (2020). Archived from the original on 30 December. (Accessed 5 September 2020).
[85] IPCC, A summary for Policy makers, in: A Report of Working Group 1 of the Inter-governmental Panel on Climate Change, Cambridge University Press, New York, 2001.
[86] J.D. Milliman, J.M. Broadus, F. Gable, Environment and economic implications of rising sea level and subsiding deltas: the Nile and Bengal Examples, Ambio 18 (6) (1989) 340–345.
[87] S.R. Khan, B. Islam, Holocene stratigraphy of the lower Ganges-Brahmaputra river delta in Bangladesh, Front. Earth Sci. China 2 (2008) 393–399, https://doi.org/10.1007/s11707-008-0051-8.
[88] S.R. Khan, Geology of barguna District, Bangladesh, Geol. Surv. Bangladesh 10 (3) (2003) 68.
[89] IPCC, Climate change synthesis report, in: Intergovernmental Panel on Climate Change, 2007. http://www.ipcc.ch/pdf/assessment-report/ar4/syr/ar4_syr.pdf.
[90] PBS, Another major cyclone, in: Bangladesh Worries about Climate Change, PBS News Hour, 2008.
[91] B. Walker, Millions in Bangladesh Exposed to Arsenic in Drinking Water, 2010. Availble at: http://www.cnn.com/2010/WORLD/asiapcf/06/20/bangladesh.arsenic.poisoning/index.html?hpt=T1.
[92] R. Nicholls, S.L. Goodbred Jr., Towards integrated assessment of the Ganges-Brahmaputra delta, in: Proceeding of the 5th International Conference on Asian Marine Geology and 1st Annual Meeting of IGCP475 Delta and APN Mega-Delta, 2004, 13 Feb.
[93] Anon, United Nations economic and social council, Progress towards the sustainable development goals report of the secretary-general, in: Archived 30 December 2020 at the Wayback Machine, High-Level Political Forum on Sustainable Development, Convened under the Auspices of the Economic and Social Council, 2020. E/2020/57. (Accessed 28 April 2020).
[94] Anon, Keigo Akimoto, Chapter 17: accelerating the transition in the context of 2 sustainable development, in: IPCC Sixth Assessment Report Mitigation of Climate Change, 2022. (Accessed 6 April 2022).
[95] M.A. Islam, A.B.K. Majlis, M.B. Rashid, Changing face of Bangladesh coast, J. NOAMI 28 (1) (2011) 1–17.
[96] M.B. Rashid, A. Mahmud, Longshore currents and its effect on kuakata beach, Bangladesh, Bangladesh, J. Geol. 29–30 (2011) 30–40.
[97] M.B. Rashid, M.A. Rahman, Coastline change and coastal islands development in the Feni estuary of Bangladesh through RS and GIS, AIMS Geosci 8 (4) (2022) 609–626, https://doi.org/10.3934/geosci.2022033.